Information-optimal phase mask design for lensless imaging

Leyla A. Kabuli, Eric Markley, and Laura Waller

Department of Electrical Engineering and Computer Sciences
University of California, Berkeley, California, USA

ABSTRACT

We use information-theoretic optimization to design phase mask encoders for lensless imaging systems. By maximizing the mutual information between objects and encoded measurements, we directly optimize the encoder for measurement quality. We explore various object sparsity levels and analyze practical trade-offs for compact systems, including sensor-to-mask distance and mask feature size. Our information-optimal designs display strong object-dependence, with sparse objects producing higher multiplexing designs. As lensless imaging systems advance towards in vivo applications, our approach provides a direct path to designing optical encoders for specific biological use cases.

Keywords: Lensless imaging, mutual information, data-driven design, phase mask design

1. INTRODUCTION

Phase mask-based lensless imaging systems use a thin optical element to capture measurements and a reconstruction algorithm to recover images. These computational imaging systems offer compact form factor and use multiplexed, one-to-many encodings to enable compressive imaging capabilities, including single-shot extended field-of-view (FOV) imaging.[1–3] Lensless imagers show promise for mesoscopy and microscopy, including emerging in vivo imaging applications.[4] However, reconstruction performance is fundamentally limited by the information encoded in measurements, requiring new phase mask designs that improve measurement quality while accounting for practical system constraints, including compactness and object-dependent performance.

Imaging system measurements can be directly optimized using information-driven techniques. Information-Driven Encoder Analysis Learning (IDEAL) optimizes encoders by maximizing the mutual information between objects and encoded measurements.[1,5,6] This approach captures the joint effects of object statistics, optical encoding, and noise, providing a comprehensive measure of encoder performance without the confounding factors introduced by reconstruction algorithms. Although this design approach is reconstruction-independent, information-optimal encoders have been empirically shown to improve reconstruction performance.[1,5]

Recent work applied information-driven design to lensless imaging, optimizing point spread functions (PSFs) for compressive extended FOV imaging using IDEAL.[1] The resulting information-optimal designs were strongly object-dependent, with encoder multiplexing levels varying with object sparsity. In this work, we extend this framework from lenslet-based PSF design to physically-constrained system design by directly designing phase masks for lensless imaging. We incorporate practical system constraints, including sensor-to-mask distance and mask feature size, and study object distributions representative of fluorescence microscopy samples. Our fabrication-aware, information-optimal phase mask designs provide a step toward object-specific, compact lensless imaging systems suitable for biological applications.

2. METHODS

We simulate lensless imaging measurements using the image formation model

$$\mathbf{y} = \mathcal{N}(\mathbf{o} * f_\theta), \tag{1}$$

Further author information: (Send correspondence to Leyla Kabuli)
Leyla Kabuli: E-mail: lakabuli@berkeley.edu

Computational Optical Imaging and Artificial Intelligence in Biomedical Sciences III, edited by Liang Gao, Guoan Zheng, Seung Ah Lee, Proc. of SPIE Vol. 13865, 1386502
2026 Published by SPIE · 1605-7422 · doi: 10.1117/12.3077933

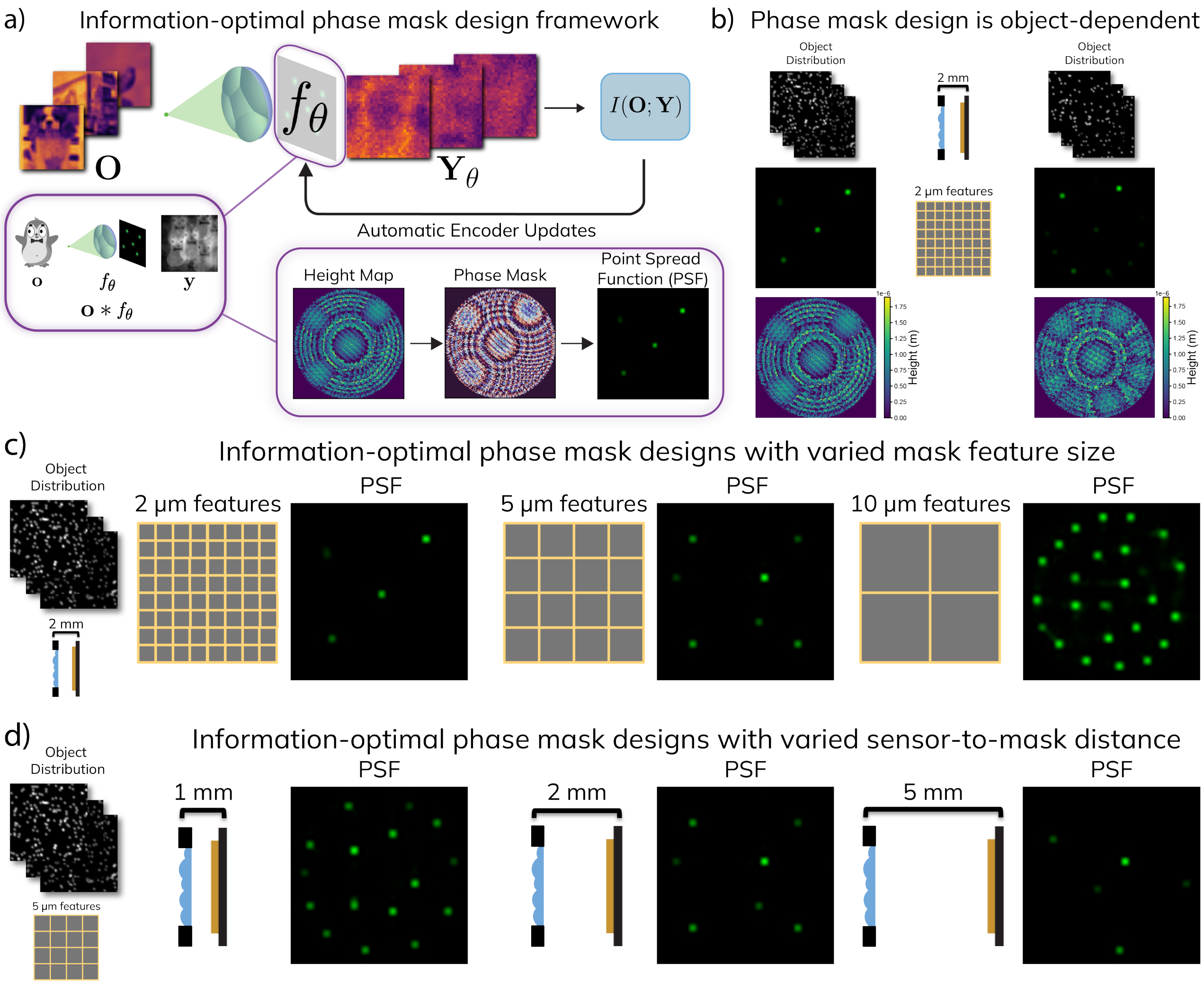

Figure 1. a) Information-optimal phase mask design based on maximizing mutual information between objects and noisy measurements. Measurements are formed by convolving objects with a point spread function (PSF) defined by a phase mask. b) The information-optimal designs for a 2 mm sensor-to-mask distance and 2 µm mask feature size are object-dependent: dense objects (left) produce PSFs with fewer focal points than sparse objects (right). c) Decreasing the mask feature size reduces the number of focal points in the PSF for a fixed sensor-to-mask distance of 2 mm. d) Increasing the sensor-to-mask distance results reduces the number of focal points in the PSF for a fixed mask feature size of 5 µm.

where $\mathbf{o}$ is the object, f_θ is the PSF generated by the system phase mask, and $\mathcal{N}$ denotes detection noise, which is modeled as signal-dependent Poisson noise applied independently to each measurement pixel.

The PSF f_θ is generated from a height map θ representing the surface profile of the phase mask following

$$f_\theta = |\mathcal{A}_z \left(\exp \left(j \frac{2\pi}{\lambda} \Delta n \theta \right) \right) |^2, \tag{2}$$

where $\mathcal{A}_z$ corresponds to angular spectrum method (ASM) propagation operator over a propagation distance of z, λ is the wavelength, and Δn is the refractive index difference between the phase mask and air.[7] We implement this physically-constrained model in JAX[8] by adapting a differentiable wave optics-based simulation framework.[9]

The surface profile of the information-optimal phase mask for a target object distribution $\mathbf{O}$ is defined by

$$\theta^* = \underset{\theta \geq 0}{\arg\max}\, I(\mathbf{O}\,;\, \mathbf{Y}_\theta)\,. \tag{3}$$

At each optimization step, the height map θ is updated to generate a new PSF f_θ, and the mutual information $I(\mathbf{O}\,;\,\mathbf{Y}_\theta)$ between the object distribution $\mathbf{O}$ and the resulting noisy measurement distribution $\mathbf{Y}_\theta$ is used as the loss function. Height map values are constrained to be non-negative, and measurements follow the image formation model in Eq. (1). The final height map θ^* corresponds to the information-optimal phase mask for the selected object distribution. This design framework is visualized in Fig. 1a.

We study object distributions consisting of fluorescent bead-like point sources with a fixed level of spatial sparsity and a mean photon count of 100 photons.[1] We quantify object sparsity using the Tamura Coefficient (TC),[10] where higher TC values correspond to sparser objects. The phase mask refractive index is $n = 1.43$ and PSFs are generated at a wavelength of $\lambda = 532\,\mathrm{nm}$. Phase masks are parameterized by 128×128 pixel height maps, corresponding to $4\times$ upsampled PSFs. For IDEAL, mutual information is estimated using a PixelCNN[5,6] fit to 4096 16×16 pixel patches, following the information-driven lensless imaging framework.[1] Each phase mask design converges within 1500 optimization steps in under 2 hours on an NVIDIA RTX A6000 GPU.

3. RESULTS

Using the information-driven phase mask design framework described above, we study the effect of practical system constraints on information-optimal lensless imaging system designs. While phase mask designs must be adjusted to object sparsity,[1] they also depend on system specifications: sensor-to-mask distance controls compactness, and mask feature size affects fabrication resolution and the quality of the resulting PSFs.

We first verify the object-dependence of information-optimal designs with physical system constraints. In Fig. 1b, we optimize phase masks for a dense object distribution (TC = 1.1064) and a sparse object distribution (TC = 1.3588), using a 2 mm sensor-to-mask distance and 2 µm mask feature size. The design optimized for dense objects produces a low-multiplexing PSF with four focal spots, whereas the sparse object distribution corresponds to a higher-multiplexing PSF with 11 focal spots, including two very faint points.

Next, we investigate the impact of mask feature size, or fabrication resolution, on phase mask designs. For a dense object distribution (TC = 1.1064) and a fixed sensor-to-mask distance of 2 mm, we optimize phase masks with feature sizes of 2 µm, 5 µm, and 10 µm (Fig. 1c). Increasing the feature size results in more PSF multiplexing. With coarse 10 µm features, the focal spots are wider than for fine 2 µm features.

Finally, we study the effect of sensor-to-mask distance, which directly controls system compactness. Using the same bead distribution as in Fig. 1c and a fixed mask feature size of 5 µm, we design phase masks for sensor-to-mask distances of 1 mm, 2 mm, and 5 mm (Fig. 1d). As the propagation distance increases, the resulting PSFs have fewer focal spots, whereas shorter propagation distances require more focal spots. This trend explains why ultra-compact lensless imaging systems require higher multiplexing, as short sensor-to-mask distances require additional mask features to distribute light across the sensor region.

4. DISCUSSION

In this work, we design physically-constrained information-optimal phase masks for lensless imaging. We verify that phase mask designs are strongly object-dependent, with more multiplexing necessary for sparse objects. We further demonstrate that practical system constraints affect phase mask designs, with shorter sensor-to-mask distances and coarser fabrication resolutions resulting in more multiplexing. Our results extend information-driven lensless imaging system design[1] by optimizing fabrication-aware phase masks. This approach provides a practical path for designing high-performance, compact, and object-specific lensless imaging systems.

Our design approach directly optimizes a height map corresponding to a freeform optical surface, rather than a lenslet-based PSF parameterization.[1] Although the only constraint imposed during optimization is height map non-negativity, the learned phase masks naturally converge to lenslet structures. The learned height map depths do not exceed 5 µm, which is compatible with existing fabrication techniques.[11] Future work can incorporate additional fabrication-specific constraints to produce freeform optical elements with smooth, slowly-varying surface profiles. While we optimize 128×128 height maps in this work, information-optimal design over a larger FOV can provide phase masks suitable for direct fabrication.

Information-optimal phase mask designs are not directly optimized for a specific downstream task. Although these designs have been shown to improve downstream reconstruction performance,[1] performance improvements are not guaranteed for specialized tasks such as classification, or for reconstruction algorithms with limited computational power. Future work can combine IDEAL with end-to-end optimization for a two-step design strategy, in which information-optimal designs can be fine-tuned to improve task performance by incorporating a specific decoder or task objective.

ACKNOWLEDGMENTS

L.A.K. was supported by the National Science Foundation Graduate Research Fellowship Program under Grant DGE 2146752. L.W. is a Chan Zuckerberg Biohub SF investigator. This work was supported by the U.S. Air Force Office Multidisciplinary University Research Initiative (MURI) program under Award No. FA9550-23-1-0281, the U.S. Air Force Office of Scientific Research under Award No. FA955-22-1-0521, and STROBE: A National Science Foundation Science & Technology Center under Grant No. DMR 1548924.

REFERENCES

[1] Kabuli, L. A., Pinkard, H., Markley, E., Hung, C. S., and Waller, L., "Designing lensless imaging systems to maximize information capture," *Optica* **13**(2), 227–235 (2026).

[2] Hung, C. S., Kabuli, L. A., and Waller, L., "Extended field-of-view lensless imaging with random multi-focal lenslet arrays," in [*Optica Imaging Congress (3D, COSI, DH, FLatOptics, IS, pcAOP)*], *Optica Imaging Congress (3D, COSI, DH, FLatOptics, IS, pcAOP)* , CTh1B.3, Optica Publishing Group (2025).

[3] Yao, X., Pathak, V., Xi, H., Chaware, A., Cooke, C., Kim, K., Xu, S., Li, Y., Dunn, T., Konda, P. C., Zhou, K. C., and Horstmeyer, R., "Increasing a microscope's effective field of view via overlapped imaging and machine learning," *Opt. Express* **30**(2), 1745–1761 (2022).

[4] Wu, J., Chen, Y., Veeraraghavan, A., Seidemann, E., and Robinson, J. T., "Mesoscopic calcium imaging in a head-unrestrained male non-human primate using a lensless microscope," *Nature Communications* (15), 1271 (2024).

[5] Pinkard, H., Kabuli, L., Markley, E., Chien, T., Jiao, J., and Waller, L., "Information-driven design of imaging systems," in [*The Thirty-ninth Annual Conference on Neural Information Processing Systems*], (2025). arXiv:2405.20559.

[6] Markley, E., Pinkard, H., Kabuli, L., Singh, N., and Waller, L., "Computationally efficient information-driven optical design with interchanging optimization," *arXiv* (2025). arXiv:2507.07789.

[7] Goodman, J. W., [*Introduction to Fourier optics*], Roberts and Company publishers (2005).

[8] Bradbury, J., Frostig, R., Hawkins, P., Johnson, M. J., Leary, C., Maclaurin, D., Necula, G., Paszke, A., VanderPlas, J., Wanderman-Milne, S., and Zhang, Q., "JAX: composable transformations of Python+NumPy programs," (2018).

[9] Sitzmann, V., Diamond, S., Peng, Y., Dun, X., Boyd, S., Heidrich, W., Heide, F., and Wetzstein, G., "End-to-end optimization of optics and image processing for achromatic extended depth of field and super-resolution imaging," *ACM Trans. Graph.* **37**(4) (2018).

[10] Tamura, H., Mori, S., and Yamawaki, T., "Textural features corresponding to visual perception," *IEEE Transactions on Systems, Man, and Cybernetics* **8**(6), 460–473 (1978).

[11] Lee, K. C., Bae, J., Baek, N., Jung, J., Park, W., and Lee, S. A., "Design and single-shot fabrication of lensless cameras with arbitrary point spread functions," *Optica* **10**(1), 72–80 (2023).